(15) B. Loev and M. M. Goodman, *Chem. Ind. (London)*, 2026 (1967).
(16) H. P. Hanson, F. Herman, J. D. Lea, and S. Skillman, *Acta Crystallogr.*, **17**, 1040 (1964).
(17) See paragraph at end of paper regarding supplementary material.
(18) M. R. Churchill, "Prospectives in Structural Chemistry", Vol. 3, J. D. Dunitz and J. A. Ibers, Ed., Wiley, New York, N.Y., 1970, p. 91.
(19) W. W. Adams and P. G. Lenhert, *Acta Crystallogr., Sect. B*, **29**, 2412 (1973).
(20) D. L. McFadden and R. T. McPhail, *J. Chem. Soc., Dalton Trans.*, 363 (1974).
(21) O. Kennard, D. G. Watson, F. H. Allen, N. W. Isaacs, W. D. S. Motherwell, R. C. Pettersen, and W. G. Towns, Ed., "Molecular Structures and Dimensions", Vol. A1, N.V.A. Oosthoek, Utrecht, Netherlands, 1972, p 52.
(22) J. T. Mague, *Inorg. Chem.*, **9**, 1610 (1970).
(23) J. T. Mague, *Inorg. Chem.*, **12**, 2649 (1973).
(24) L. R. Bateman, P. M. Maitlis, and L. F. Dahl, *J. Am. Chem. Soc.*, **91**, 7292 (1969).
(25) S. Brückner and L. Randacclo, *J. Chem. Soc., Dalton Trans.*, 1017 (1974).
(26) N. K. Hota, H. A. Patel, A. J. Carty, M. Mathew, and G. J. Palenik, *J. Organomet. Chem.* **32**, C55 (1971).
(27) V. G. Albano, P. L. Bellon, and G. Cianl, *J. Organomet. Chem.*, **38**, 115 (1972).
(28) A. Nakamura and N. Hagihara, *Bull Chem. Soc. Jpn.*, **34**, 452 (1961).
(29) M. D. Rausch and R. A. Genetti, *J. Org. Chem.*, **35**, 3888 (1970).
(30) S. A. Gardner, H. B. Gordon, and M. D. Rausch, *J. Organomet. Chem.*, **60**, 179 (1973).

Kinetic Study of the Copper(II)-Catalyzed Enolization, Ketonization, and Decarboxylation of Oxaloacetate[1]

N. V. Raghavan and D. L. Leussing*

Contribution from the Department of Chemistry, The Ohio State University, Columbus, Ohio 43210. *Received December 4, 1974*

Abstract: Cu(II) and oxaloacetate, $oxac^{2-}$, react rapidly in solution to form $Cu(oxac)_{keto}$ which enolizes and decarboxylates via competing reaction paths. Because the two processes proceed at comparable rates, and enolization is reversible, the evolution of CO_2 from these reaction mixtures is observed to be biphasic, the slower rate limited by the reketonization of $Cu(oxac)_{enol}$. In this respect catalysis by Cu(II) differs from that reported for other metal ions where only the slower step has been observed. The presence of a fast decarboxylation step has made it possible to obtain the true rate constant for the decarboxylation of $Cu(oxac)_{keto}$ and also to observe the reaction kinetics of the short-lived intermediate, $Cu(pyr)_{enolate}$ (pyr = pyruvate). Evaluation of the equilibrium constant for the reaction $Cu(oxac)_{keto} \rightleftharpoons Cu(oxac)_{enol}$ is also made possible by the biphasic nature of CO_2 evolution. The consumption of H^+ which accompanies the conversion of the intermediate to Cu(pyr) was also found to be biphasic, the rate at shorter times depending on the kinetics of pyruvate formation and at longer times, like slow CO_2 evolution, being determined by the reketonization of $Cu(oxac)_{enol}$. A proton-catalyzed and an uncatalyzed reaction path were found for the enolization of $Cu(oxac)_{keto}$. The rate of protonation of $Cu(pyr)_{enolate}$ was found to be independent of pH, indicating that Cu(II)–oxygen bond breaking associated with ligand rearrangement is rate limiting. Inhibition of decarboxylation at high Cu(II) concentrations arises from the formation of polynuclear Cu(II) complexes of $oxac_{enolate}^{3-}$. A detailed quantitative description of the reaction system has been obtained and is reported.

Similarities between enzymatic and metal ion catalyzed decarboxylation processes have for a number of years stimulated investigations of the metal ion catalyzed reactions with the hope of shedding light on the enzymatic systems.[2-9] Detailed studies have focused mainly on the decarboxylation of oxaloacetic acid (H_2oxac) and its derivatives.[10-18] Metal ion-oxaloacetate complexes lose CO_2 to form a complex of pyruvate enolate, **2**. This latter species

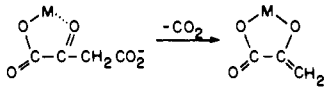

1 2

rearranges and acquires a proton to form pyruvate, **3**.[10-18] A competitive reaction with decarboxylation comprises the

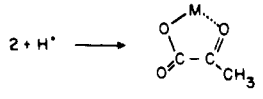

3

formation of $oxac_{enol}^{2-}$,[4-11] which does not decarboxylate.[11-17]

In studying the decarboxylation of α,α-dimethyloxaloacetate, Steinberger and Westheimer[11] noted that a biphasic absorbance change occurs in the ultraviolet region. Since α,α-dimethyloxaloacetate cannot enolize, an initial increase in absorbance was attributed to the formation of the immediate decarboxylation product, the dimethyl derivative of pyruvate enolate. The succeeding absorbance decrease was then assigned to protonation and ketonization of the intermediate. A similar sequence of absorbance changes is noted for the metal ion catalyzed decarboxylation of $oxac^{2-}$; however, the enolization of $oxac^{2-}$ itself complicates the interpretation. Gelles and Hay[12] and Gelles and Salama[13] claim that $oxac^{2-}$ enolization is fast compared to the CO_2 loss so that the observed absorbance changes arise from the Steinberger-Westheimer reaction sequence. Others have ascribed these changes to the formation of $oxac^{2-}$ enol and enolate complexes[4,14,16] which ultimately disappear as decarboxylation proceeds.

Until a recent quantitative study of the influence of Zn(II) on the $oxac^{2-}$ reactions appeared[18] very little had been reported regarding the influence of metal ions on the enolization rates. It was shown[18] that an increase in uv absorbance which is complete in about 30 s after mixing Zn(II) and $oxac^{2-}$ solutions arises from the conversion of $Zn(oxac)_{keto}$ (**1**) to $Zn(oxac)_{enol}$ (**4**). A subsequent slower absorbance decrease proceeds at the same rate as CO_2 loss. The protonation of intermediate $Zn(pyr)_{enolate}$ (**2**) is sufficiently fast that it is rate limited by decarboxylation and is not observed. Thus, the reaction sequence found by Steinberger and Westheimer does not account for the absorbance changes in the Zn(II)-$oxac^{2-}$ systems. Because the rate of decarboxylation is relatively slow, enolization essentially comprises a preequilibrium step, and therefore, as Gelles

and his co-workers clearly recognized,[12,13] the absolute value of the rate constant for the decarboxylation of $Zn(oxac)_{keto}$ is not directly accessible from kinetic determinations alone.

In marked contrast, it was found in the present study that the behavior of the Cu(II) reaction system is considerably more complicated than the Zn(II) reaction system. The intrinsic rate of decarboxylation of $Cu(oxac)_{keto}$ has been found to be similar to the enolization rate. Therefore, when solutions of Cu^{2+} and $oxac^{2-}$ are mixed, $Cu(oxac)_{keto}$ disappears via competing enolization and decarboxylation paths. After about 30 s the concentration of $Cu(oxac)_{keto}$ is reduced to a low level and further CO_2 evolution must wait for the reconversion of $Cu(oxac)_{enol}$ to $Cu(oxac)_{keto}$. The observation of a biphasic evolution of CO_2 permitted the evaluation of the absolute rate constant for the decarboxylation of $Cu(oxac)_{keto}$. An additional bonus, resulting from the presence of the initial fast decarboxylation reaction, was the discovery that it is possible to observe and measure the rate of proton uptake which occurs during the ketonization of $Cu(pyr)_{enolate}$, reaction **2** → **3**. Thus, it was possible to gain valuable information regarding the lifetime and kinetics of disappearance of this reactive intermediate.

A preliminary communication of these results has been reported.[19] Full details and additional data are now described.

Experimental Section

Materials. Oxaloacetic acid, obtained from Nutritional Biochemical Corporation, Cleveland, Ohio, was determined by titration with standardized NaOH to be 97.7% pure. It was stored under refrigeration and used without further purification. Stock solutions were prepared by weight immediately before use. Copper(II) chloride stock solutions were prepared from J. T. Baker Chemical Co. reagent grade material and analyzed by the method of Schwarzenbach and Flaska.[20] Lactic acid dehydrogenase (rabbit muscle) was obtained from Nutritional Biochemical Corporation and NADH was obtained from Calbiochem. Dilute acetic acid, sodium hydroxide, and potassium chloride solutions were prepared in the usual manner. Doubly distilled and deionized water was used throughout.

For the kinetic runs, two reaction solutions, one of Cu(II) and the other of oxaloacetate, were prepared for each experiment by measuring appropriate volumes of the stock solutions into two 100-ml volumetric flasks. Both of the solutions were buffered using a low level of acetic acid. Base was added to adjust the solutions to the desired pH. The ionic strength was maintained at 0.1 by the addition of suitable amounts of KCl. All experiments were run at 25°. After mixing the reaction solutions, measurements of CO_2 pressure, absorbance, or H^+ ion consumption were begun as soon as possible consistent with the limitations of the apparatus being employed.

Three distincally different rate processes were found depending on the physical property being measured. These are illustrated in Figure 1 where the generalized ordinate is linear in the physical quantity designated in the legend. Because the rate data were analyzed by determining the relaxation time as each reaction approached equilibrium, it was not necessary to know the absolute values of absorbance, pressure, or H^+ ion consumption as a function of time; a sufficient condition was that the measured responses were linear in these quantities. Also, because the slow and fast steps in a run were usually sufficiently separated in time so that they could be logged separately, relaxation times, τ_i, were generally obtained from the data by a least-squares fit of the data to a simple exponential decay equation of the form,

$$R_t = R_\infty + R_1 e^{-t/\tau_1}$$

where R_t is the measured response at time t, R_∞ is the value at the completion of the reaction, and R_1 is the amplitude. Under the concentration conditions employed to obtain the data shown in Figure 1, practically all of the $oxac^{2-}$ is bound as Co(oxac).

The fastest of the observed rates, designated here as τ_1, was

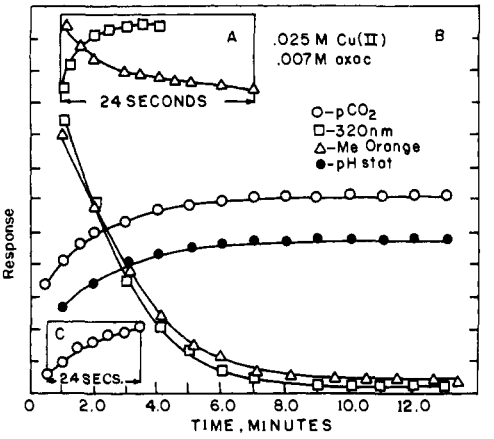

Figure 1. Relative response vs. time curves for the decarboxylation and enolization of Cu(II) oxaloacetate. The values of the ordinate are: ○, pressure of CO_2; □, absorbance at 320 nm in the absence of methyl orange; △, absorbance at 514 nm of the acid form of methyl orange, $pH_{initial}$ 3.4; ●, volume of 0.1006 M HCl, pH-stat titration at pH 3.19.

complete in about 30 s and was followed primarily by monitoring absorbance increases in the region 280-320 nm. Typical data are shown as the open squares of inset A in Figure 1. A Durrum-Gibson stopped flow spectrophotometer interfaced to a Nova minicomputer was used to log the data. For most of these experiments the total concentrations of reactants in the mixed solutions lay in the range $(1.0\text{-}130) \times 10^{-4}$ M Cu(II), $(5.0\text{-}20.0) \times 10^{-3}$ M acetate, and $(1.0\text{-}5.0) \times 10^{-4}$ M oxaloacetate.

A Cary 14 spectrophotometer, equipped with a thermostated cell compartment, was used to record the slow uv absorbance decreases, which are designated as τ_3 and are illustrated as the open squares of inset B, Figure 1. For most of these experiments the total concentrations of reactants in the final reaction mixture were in the range $(1.0\text{-}26.0) \times 10^{-3}$ M Cu(II), $(5.0\text{-}20.0) \times 10^{-3}$ M acetate, and $(1.0\text{-}2.0) \times 10^{-4}$ M oxaloacetate. The pH changes monitored during the reaction under these concentration conditions were found to be less than 0.03 pH unit from beginning to end.

During the ketonization of pyruvate enolate, **2** → **3**, a proton is acquired causing an increase in pH that can be used to follow this step. Absorbance changes at 514 nm of the acid form of methyl orange in unbuffered reaction solutions were examined. A biphasic pH change was uncovered and is shown as open triangles in Figure 1. The faster process (inset A) shows a relaxation time, τ_2, which lies between τ_1 and τ_3. The amount of H^+ consumed in the τ_2 phase, ΔH_2, relative to the total amount consumed by the end of the reaction, ΔH_∞, should give the relative amount of pyruvate formed in the initial stages of the reaction. The H^+ consumed can be determined from the absorbance changes of methyl orange using the equation,

$$\frac{\Delta H_2}{\Delta H_\infty} = \frac{([H^+]_0 - [H^+]_2)}{([H^+]_0 - [H^+]_\infty)} = \left(\frac{A_0 - A_1}{A_0 - A_\infty}\right)\left(\frac{1 + \beta_{MO}(H^+)_2}{1 + \beta_{MO}(H^+)_\infty}\right)$$

where $[H^+]_0$ is the hydrogen ion concentration at zero time, $[H^+]_2$ is the hydrogen ion concentration at the end of the τ_2 phase and $[H^+]_\infty$ is the hydrogen ion concentration at infinite time. A_0, A_1, and A_∞ are the corresponding values determined for the absorbance and β_{MO} is the protonation constant of methyl orange. For this last quantity a value of 2.90×10^3 was used.[21] In experiments on mixtures initially at pH 3.4 it was found that $\Delta H_2/\Delta H_\infty$ is about 1:4; that is, about 20% of the H^+ required to form pyruvate is consumed in the reactions manifested in the τ_2 phase.

The rate of hydrogen ion consumption was also followed using a pH-stat. A Radiometer pH-stat equipped with an ABU-1 autoburet was used. Owing to the relatively slow response of the instrument, only the slow relaxation could be followed using this technique. An aliquot of a $Cu^{II}Cl_2$ solution was added rapidly to an oxaloacetic acid-potassium chloride solution contained in the pH-stat cell. The pH-stat was set to the desired pH and, as $Cu^{II}pyr$ was formed, the pH of the solution was maintained constant at pH 3.19 by automatic addition of the titrant, a standard HCl solution. The volume of added titrant with respect to time was recorded.

The rate of uptake of HCl in inset B of Figure 1 is seen to agree closely with the rate of the slower changes observed using methyl orange. At the end of the reaction, it was found that 1 mol of $oxac^{2-}$ required 0.85–0.90 mol of proton, consistent with 1:1 stoichiometry between $oxac^{2-}$ and pyruvate, the reaction product. A possible side reaction which may account for the slightly low results is the formation of an enolate complex of parapyruvate (the dimer of pyruvate),[22] $2Cu^{2+} + oxac^{2-} + pr^- \rightarrow Cu_2(O_2CC(O)(CH_3)CH_2COCO_2)^+ + CO_2$.

Pressure changes due to CO_2 evolution were followed in a sealed reaction system connected to a Texas Instrument Precision Pressure Gauge, Model 145-01. The reaction solutions were shaken vigorously, and the output of the gauge was continuously monitored with a Hewlett-Packard 7101 BM strip chart recorder. A biphasic rate of CO_2 evolution was observed when buffered Cu(II) and $oxac^{2-}$ solutions were mixed in the apparatus. These two phases are shown in insets B and C of Figure 1. A tendency for slow nucleation caused difficulties in measuring the faster rate of CO_2 evolution and prevented an accurate evaluation of the relaxation time of the faster process, but it was observed to be similar to, but with a tendency to be slightly slower than, the value of τ_1 obtained from stopped flow. Qualitatively, the fast CO_2 evolution rates respond in the same manner to changes in solution composition as do the fast rates measured spectrophotometrically. There is little doubt, therefore, that these two physical processes are associated with the same set of chemical reactions. Nucleation difficulties did not interfere with the pressure measurements made during the slow CO_2 evolution step. It was found that these rates agree, within the experimental deviations, with those found from slow absorbance and H^+ ion consumption measurements under similar experimental conditions.

The amount of CO_2 evolved in the fast step relative to the total amount evolved when all of the $oxac^{2-}$ has been decarboxylated at pH 3.4 by excess of Cu(II) was obtained by recording complete p_{CO_2}-time curves from the time of mixing until CO_2 evolution ceased and a constant pressure was attained. The ratio of the pressure change associated with the first step to the total pressure change found at the end of the reaction showed that about 18% of the total available CO_2 is released during the first phase. This figure gives an independent check of the value obtained from H^+ consumption measurements for the amount of pyruvate formed initially.

The amount of pyruvate formed 25 s after mixing was determined directly by an enzymatic assay using the procedure described by Meister.[23] Ten milliliters of 5.0×10^{-2} M $CuCl_2$ solution was mixed rapidly with 10 ml of 4.0×10^{-3} M oxaloacetate solution at pH 3.42 and the reaction was quenched after 25 s by cooling in ice and adding 20 ml of EDTA solution (0.1 M) along with 10 ml of phosphate buffer (pH 7.10). One milliliter of the reaction mixture was transferred to an optical cuvette containing 1.0 ml of phosphate buffer and 0.2 ml of NADH, and the absorbance at 340 nm was recorded. The pyruvate was assayed by the decrease in absorbance on the addition of 1 μl of lactate dehydrogenase (1.0 unit).[23] In a replicate solution the same procedure was carried out to assay the pyruvate formed after the reaction has gone to completion. After correcting for a blank, the ratio of the initial phase of the reaction to the total formed at completion was found to be 0.22.

Potentiometric titrations of $oxac^{2-}$ in the presence and absence of Cu(II) were made under conditions in which decarboxylation is inhibited. A weighed quantity of oxaloacetic acid was dissolved in water and a NaOH solution was added until the pH of the solution reached 12.0. At this pH decarboxylation does not occur owing to enolate formation.[12,13] The ionic strength of an aliquot of the solution was adjusted to 0.1 M by the addition of KCl and the resulting mixture was titrated rapidly with 0.1006 M HCl. Another aliquot was treated in the same way except a known amount of Cu(II) was added just before the rapid titration. The two titration curves are shown in Figure 2. Both curves show an end point in the region of pH 7–8. This corresponds to the titration of the excess NaOH and $oxac^{2-}$ enolate. In the presence of Cu(II), the curve is displaced to more acidic values owing to the release of H^+, or the consumption of OH^-. Below pH 6 the displacement corresponds to the release of 1 mol of H^+ per mole of Cu^{2+}, indicating the formation of either an enolate complex, $(CuH_{-1}oxac)_n^{n-}$, or a hydroxy complex, $(Cu(OH)oxac)_n^{n-}$. For reasons given below, the preferred formulation is that of a dimeric enolate. The titration data between pH 3.0 and 5.0 were analyzed numerically, and the equilibrium constant for the reaction $2Cu^{2+} + 2oxac^{2-} \rightleftarrows Cu_2H_{-2}oxac_2 + 2H^+$ was evaluated to be 27 ± 3 M^{-1}. Above pH 6.0, species containing a number of hydroxide groups per Cu(II) appear to be formed. These data were not analyzed.

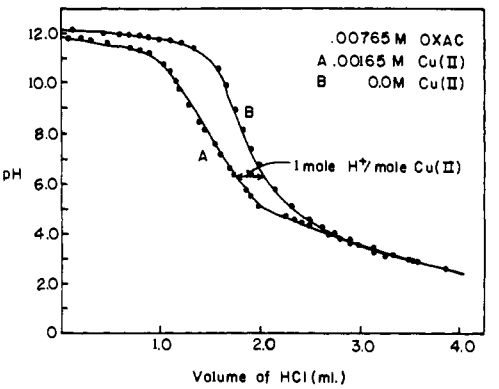

Figure 2. Titration of alkaline solutions of oxaloacetate in the presence and absence of Cu(II): volume initial = 16.00 ml; 0.1006 Ml.

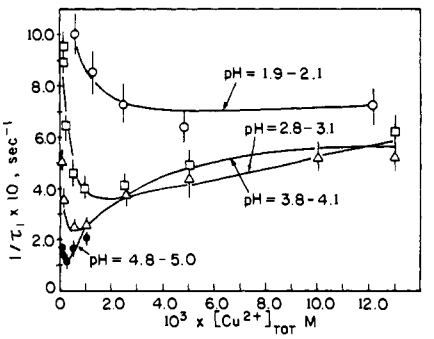

Figure 3. The fastest relaxation as a function of total Cu(II) concentration and pH. Rates measured spectrophotometrically in the uv region. The solid lines are theoretical.

Results

After mixing Cu(II) and $oxac^{2-}$ solutions, three distinct rate processes are observable in measurements of uv absorbance, CO_2 pressure, and H^+ ion consumption. All of these different types of measurements show biphasic changes. The fastest process, τ_1, is discernible in uv absorption and CO_2 release experiments; an intermediate rate process, τ_2, is manifested in H^+ consumption experiments; and, the slowest process, τ_3, is revealed in slow changes observed for all three of these different types of measurements, and all show essentially the same slow decay rates.

Under the experimental conditions employed in this investigation 86–92% of the $oxac^{2-}$ is present initially in the keto form.[24,25] Measurements of the amount of CO_2 evolved, H^+ ion consumed, and pyruvate formed in the first phase of the reaction agree remarkably well and show that in the presence of excess Cu(II) at pH 3.2–3.4, 18, 20, and 22%, respectively, the $oxac_{keto}^{2-}$ is relatively rapidly decarboxylated and converted to pyruvate. The remaining 80% of the $oxac^{2-}$ is converted to enol and enolate complexes of Cu(II).

The fastest relaxation, τ_1, shows a rather complicated pH and Cu(II) concentration dependence. This can be seen in Figure 3 where $1/\tau_1$ is plotted vs. the total Cu(II) concentration for experiments run at various pH. Similar curves, which did not show the minima, were found earlier for the ketonization/enolization processes in $Zn(II)$-$oxac^{2-}$ solutions.[18] Using the results of this earlier work as a guide and

the computational procedures described therein, it was possible to obtain iteratively the constants for the rate equations which were found to apply to the reaction system. The reactions are summarized below in Scheme I.

Scheme I

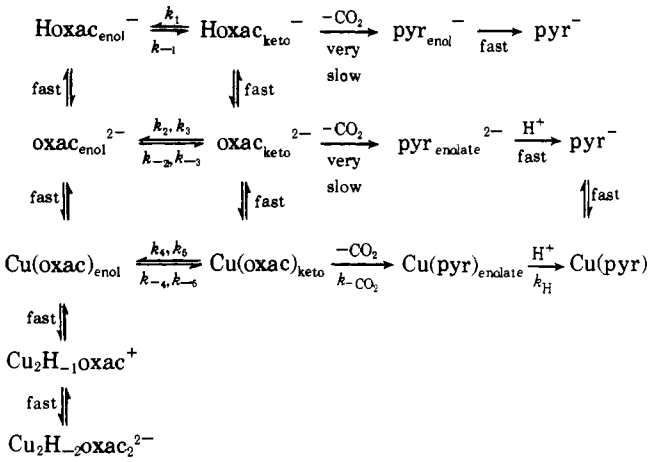

On mixing a metal-ion-free $oxac_{keto}^{2-}$ solution with Cu(II), $Cu(oxac)_{keto}$ is very rapidly formed and then disappears at a measurable rate via decarboxylation and enolization paths. This combination of events gives rise to the first relaxation, τ_1. The slower relaxation that is associated with CO_2 evolution, τ_3, arises from the decarboxylation of the low steady state concentration of $Cu(oxac)_{keto}$ that remains. The concentration of this reactant is replenished via the reketonization of $Cu(oxac)_{enol}$. The protonation of intermediate $Cu(pyr)_{enolate}$ is sufficiently fast compared to its rate of generation that it does not contribute appreciably to the absorbance during the last phase. Thus, the absorbance changes, H^+ consumption, and CO_2 evolution all show the same relaxation rate, $1/\tau_3$. The τ_1 and τ_3 data were analyzed together.

The rates by which these two processes approach their steady state values were found through trial and error to be described by the relaxation equations,

$$-\frac{d\delta oxac_{keto,\Sigma}}{dt} = A\delta oxac_{keto,\Sigma} - B\delta oxac_{enol,\Sigma} + k_{-CO_2}f_{Cu(oxac),keto}\delta oxac_{keto,\Sigma} = \frac{1}{\tau_i}\delta oxac_{keto,\Sigma} \quad (1)$$

$$-\frac{d\delta oxac_{enol,\Sigma}}{dt} = -A\delta oxac_{keto,\Sigma} + B\delta oxac_{enol,\Sigma} = \frac{1}{\tau_i}\delta oxac_{enol,\Sigma} \quad (2)$$

$$A = k_1[H^+]f_{Hoxac,keto} + (k_2[H^+] + k_3[HOAc])f_{oxac,keto} + (k_4[H^+] + k_5)f_{Cu(oxac),keto} \quad (3)$$

$$B = k_{-1}[H^+]f_{Hoxac,enol} + (k_{-2}[H^+] + k_{-3}[HOAc])f_{oxac,enol} + k_{-4}[H^+] + k_{-5})f_{Cu(oxac),enol} \quad (4)$$

$$oxac_{keto,\Sigma} = H_2oxac_{keto} + Hoxac_{keto}^- + oxac_{keto}^{2-} + Cu(oxac)_{keto}$$

$$oxac_{enol,\Sigma} = H_2oxac_{enol} + Hoxac_{enol}^- + oxac_{enol}^{2-} + Cu(oxac)_{enol} + Cu_2H_{-1}oxac_{enol}^+ + 2Cu_2H_{-2}oxac_2^{2-}$$

Here $f_{x,keto/enol}$ represents the fraction of the keto or enol form of $oxac^{2-}$ present as species x, e.g.

$$f_{oxac^{2-},keto} = \frac{[oxac_{keto}^{2-}]}{oxac_{keto,\Sigma}}$$

The values of $f_{x,keto/enol}$ are determined by solving the set of equations based on the mass balance of Cu_{tot} and $oxac_{tot}$, the macroequilibrium constants, the pH, and the microscopic equilibrium constants for the enolization of the various $oxac^{2-}$ species. The formation constants of $Hoxac^-$ and H_2oxac were determined in separate experiments and the enol/keto ratios of $oxac^{2-}$, $Hoxac^-$, and H_2oxac have been estimated.[24] The formation constant of the enolate dimer, $Cu_2H_{-2}oxac_2^{2-}$, was also determined separately.

The backward rate constants in eq 1, 2, and 4 are equal to the quotients of the forward rate constants and the corresponding microscopic enolization equilibrium constant. Values of k_2 and k_3 have been reported earlier.[18]

In analyzing the rate data it was found that the only additional complexes required to describe the rate behavior were Cu(oxac) and $Cu_2H_{-1}oxac^+$. Complexes analogous to these were found in the Zn(II) system.[18] The latter complex is an enolate, but the enol/keto ratio of the former is unknown. Owing to the biphasic nature of the CO_2 evolution in this system it was possible to determine this ratio and also to evaluate the microscopic rate constants appearing in eq 1, 2, 3, and 4.

Three independent measurements of the extent of pyruvate formation during the first phase of the reaction at pH ~3.4 in the presence of excess Cu(II) indicate that about 20% decarboxylation occurs initially with the remaining 80% accounted for by enolization. Under these reaction conditions the rate behavior is simplified because only paths involving Cu(oxac) need be considered. The percent decarboxylation is then related simply to the rate constants by the expression,

$$\% \text{ decarboxylation} = \frac{k_{-CO_2}}{k_4[H^+] + k_5 + k_{-CO_2}} \times f_{keto} \times 100 \quad (5)$$

where, f_{keto} is the fraction of total $oxac^{2-}$ initially present in the keto form. The value of k_{-CO_2} may be related to those of k_4, k_5, and k_{enol} by imposing the constraint that 20% decarboxylation was observed at pH 3.4.

Equations 1-4 predict two relaxations which are eigenvalues of the matrix,

$$\begin{vmatrix} A + k_{-CO_2}f_{Cu(oxac),keto} - \frac{1}{\tau_i} & -B \\ -A & +B - \frac{1}{\tau_i} \end{vmatrix} \quad (6)$$

The larger root corresponds to the faster relaxation and the smaller root to the slower relaxation.

The iterative solution was started by first estimating a value of k_{enol}, for the reaction $Cu(oxac)_{keto} \rightleftharpoons Cu(oxac)_{enol}$, and while holding this invariant determining the "best" least-squares fit of the remaining unknowns in eq 6 to the τ_1 data. A nonlinear least-squares curve fitting program[18] was used to perform this task.

The constants so found were then held invariant while the τ_3 data were used to obtain a better value of k_{enol}. Two alternate course of action are available to achieve this. Either eq 6 may be used once again, but using the τ_3 data, or the steady state approximation may be invoked given the relationship,

$$\frac{1}{\tau_3} = k_{-CO_2}f_{Cu(oxac),keto}\frac{B}{A + k_{-CO_2}f_{Cu(oxac),keto}} \quad (7)$$

where the terms A, B, and $f_{Cu(oxac),keto}$ are functions of k_{enol}. Both approaches yield essentially the same results.

Table I. Rate and Equilibrium Constants for Decarboxylation and Enolization (I = 0.1, 25°)

A. Overall Formation Constants

Reaction	Log β
$oxac^{2-} + H^+ \rightleftarrows Hoxac^-$	3.996
$oxac^{2-} + 2H^+ \rightleftarrows H_2oxac$	5.924
$oxac^{2-} + Cu^{2+} \rightleftarrows Cu(oxac)$	4.16
$oxac^{2-} + 2Cu^{2+} \rightleftarrows Cu_2H_{-1}oxac^+ + H^+$	2.550
$2oxac^{2-} + 2Cu^{2+} \rightleftarrows Cu_2H_{-2}oxac^{2+} + 2H^+$	1.43
$oxac^{2-} + Zn^{2+} \rightleftarrows Zn(oxac)$	2.412
$oxac^{2-} + 2Zn^{2+} \rightleftarrows Zn_2H_{-1}oxac^+ + H^+$	−1.134

C. Decarboxylation Constants

Species	$10^3 k_{-CO_2}$ (s^{-1})
$oxac^{2-}$	0.0166[c]
$Hoxac^-$	0.0566
H_2oxac	0.00106
$Cu(oxac)_{keto}$	170
$Zn(oxac)_{keto}$	47
$Mg(oxac)_{keto}$	2.2[d]

B. Enolization Constants

i	Reaction	K_{enol}	k_i, M^{-1} s^{-1} or s^{-1}	k_{-i}, M^{-1} s^{-1} or s^{-1}
1	$Hoxac_{keto}^- + H^+ \rightleftarrows Hoxac_{enol}^- + H^+$	0.122[a]	7.5	62
2	$oxac_{keto}^{2-} + H^+ \rightleftarrows oxac_{enol}^{2-} + H^+$	0.164[a]	1.38×10^3	8.4×10^3
3	$oxac_{keto}^{2-} + HOAc \rightleftarrows oxac_{enol}^{2-} + HOAc$	0.164[a]	5.7	34.8
4	$Cu(oxac)_{keto} + H^+ \rightleftarrows Cu(oxac)_{enol} + H^+$	12	2.8×10^2	30
5	$Cu(oxac)_{keto} \rightleftarrows Cu(oxac)_{enol}$	12	0.41	0.04
6	$Zn(oxac)_{keto} + H^+ \rightleftarrows Zn(oxac)_{enol} + H^+$	5	1.5×10^3	300
7	$Zn(oxac)_{keto} + HOAc \rightleftarrows Zn(oxac)_{enol} + HOAc$	5	6.3	1.2
8	$Zn(oxac)_{keto} \rightleftarrows Zn(oxac)_{enol}$	5	0.19	0.035
9	$Zn(oxac)_{keto} + OAc^- \rightleftarrows Zn(oxac)_{enol} + OAc^-$	5	7.5	1.4

[a] Reference 24. [b] Not corrected for k_{-CO_2}. [c] Reference 13. [d] Determined by W. D. Covey in our laboratories.

This sequence of computations was repeated until further improvements in the sum squares of the deviations became insignificant. The rate and equilibrium constants so obtained are presented in Table I. The solid lines shown in Figures 3 and 4 are the theoretical curves calculated using these results. The excellent agreement which has been achieved between the complicated observed and theoretical curves for both the fast and slow processes lends strong support to the present interpretation.

At low concentration levels of Cu(II), the rates shown in Figure 3 are seen to decrease rapidly as the Cu(II) concentration increases. The relatively fast rates which are observed at a zero concentration level of Cu(II) arise from the acid catalyzed enolization/ketonization reactions of $oxac^{2-}$. These rates become slower as $oxac^{2-}$ is converted to Cu(oxac), which reacts at a slower rate. The increase in rate which accompanies further increases in the Cu(II) levels arises from the complicated interplay that the formation of the various Cu(II) complexes has on the various terms in the relaxation equations 1 and 2.

The path designated as k_1 in Scheme I and Table I is assigned to the proton catalyzed enolization of $Hoxac_{keto}^-$. This path was not observed in the Zn(II) study[18] owing to the fact that the pH range studied did not extend to as low values as employed here. The k_4 path is assigned solely to the proton catalyzed enolization of $Cu(oxac)_{keto}$ by analogy to the behavior of $Zn(oxac)_{keto}$[18] and from the observations that the slow Cu(II) catalyzed rates of CO_2 evolution show little H^+ dependence, except perhaps under highly acidic conditions.[10,12,13]

The term k_5 arises from enolization pathways of $Cu(oxac)_{keto}$ that show neither acid nor base catalysis. This term is found to be much more important with Cu(II) than with Zn(II), and actually in the original analysis of the Zn(oxac) data[18] this term was overlooked.[26] With excess Cu(II) this path becomes important at values of pH greater than 3.

The second relaxation, τ_2, arises from a reaction in which H^+ ions are consumed and must, therefore, be assigned to the process,

$$Cu(pyr)_{enolate} + H^+ \xrightarrow{k_H} Cu(pyr)^+$$

Experimental values of the reciprocal of τ_2, shown in Table II, are seen to be pH independent under the conditions studies. The value of k_H for the first-order process is then simply taken as the average of the values given in Table II, 0.3 s^{-1}. The zero-order dependence on H^+ concentration indicates that Cu(II)-enolate oxygen bond breaking comprises the rate limiting process.

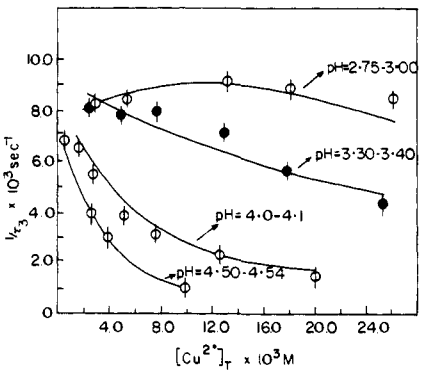

Figure 4. The slowest relaxation as a function of total Cu(II) and pH. Rates measured spectrophotometrically in the uv region. The solid lines are theoretical.

Table II. The Reciprocal of the Faster Relaxation Times ($1/\tau_2$) Observed for the Decay of the Acid Form of Methyl Orange (T = 25°; I = 0.1)

No.	$10^2[Cu^{2+}]_{tot}$, M	$10^4[oxac]_{tot}$, M	$pH_{initial}$	$1/\tau_2$, s^{-1}
1	2.0	7.42	3.605	0.32
2	2.50	8.13	3.391	0.31
3	2.50	7.41	3.295	0.31
4	2.50	8.14	3.395	0.30
5	2.50	8.13	3.895	0.30
6	2.50	8.13	4.395	0.28

Discussion

The reactions that have been described in this work are summarized in Scheme I.

Gelles and Salama[13] report a potentiometrically determined value of the formation constant of Cu(oxac) which had been extrapolated to zero ionic strength using the Davies equation. Back-calculation yields a value of $10^{4.0}$ for I = 0.1, 25°. This result is in excellent agreement with our kinetically determined value of $10^{4.12}$ for the same conditions.

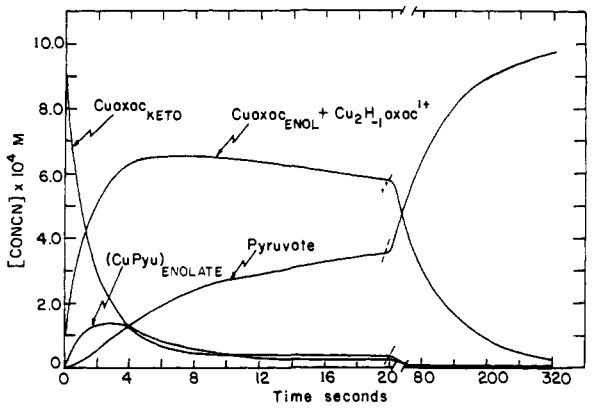

Figure 5. Concentration-time profiles in the Cu^{2+}-$oxac^{2-}$ system: $(Cu^{2+})_{tot}$ = 0.025 M; $oxac^{2-}$ = 0.001 *M*; pH 3.4.

The equilibrium constant found here for the formation of Cu(oxac), $10^{4.0}$, is 1.6 log units greater than that reported earlier[18] for the formation of Zn(oxac), $10^{2.4}$. The magnitudes of these constants and their difference are surprisingly high compared to the behavior of analogous ligands. $oxac^{2-}$ is coordinated predominantly in the enol form with both Cu(II) and Zn(II), and molecular models show that $oxac_{enol}^{2-}$ can be bound as a five-membered ring, **4a,** a six-membered ring, **4b,** or a seven-membered ring, **4c.** Maleate

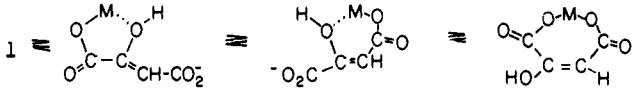

4a 4b 4c

is a good model ligand for **4c,** and the values of β_1 for the Zn(II) and Cu(II) maleates are listed[27] respectively as $10^{2.0}$ and $10^{3.4}$ for conditions comparable to those employed here. There are not as satisfactory model ligands for the hydroxy coordinated structures **4a** and **4b.** In enol coordination the constraints imposed by the carbon-carbon double bond angles prevent both carboxylate groups from simultaneously coordinating and force the ligand to be bound bidentately to the metal ion. A possible analogue of structure **4a,** malic acid, forms complexes with Zn(II) and Cu(II) that are very similar in their stabilities[27] to those found in this series, but molecular models show that malic acid can actually function as a tridentate ligand in which both carboxylate groups and the hydroxy group are coordinated. Other ligands such as lactate and 3-hydroxypropionate form considerably weaker complexes[20] than have been found in these studies, although the difference is greater with Cu(II) than it is with Zn(II); the formation constant of $Zn(lac)^+$ is about $10^{2.0}$ M^{-1} and that of $Cu(lac)^+$ is about $10^{2.5}$ M^{-1}.[27] While these comparisons do not provide a definitive picture, they do suggest that the highly stable $Cu(oxac)_{enol}$ complex is present predominantly as structure **4c,** but $Zn(oxac)_{enol}$ probably contains a larger proportion of **4a** and **4b.**

The Cu(II) catalyzed decarboxylation of $oxac^{2-}$ displays a rate law which occupies an interesting intermediate position between that observed by Steinberger and Westheimer[11] for the Cu(II) catalyzed decarboxylation of α,α-dimethyloxaloacetate and that found for the Zn(II) catalyzed decarboxylation of $oxac^{2-}$.[18] In the former reaction, enolization of the substrate cannot occur and the intermediate enolate of the substituted pyruvate is sufficiently stable to be observable for a relatively long period of time. In the latter reaction, $oxac^{2-}$ enolization is fast compared to decarboxylation, so that the rate limiting step in CO_2 loss is determined indirectly by the rates of enolization and reketonization of the $oxac^{2-}$. Furthermore, the lifetime of the intermediate $Zn(pyr)_{enolate}$ is sufficiently short compared to its rate of generation that it is not observable spectrophotometrically. With Cu(II) the absolute value of the decarboxylation rate constant is sufficiently high that appreciable $Cu(oxac)_{keto}^{2-}$ decarboxylation occurs concurrently with enolization when Cu(II) and $oxac^{2-}$ solutions are first mixed. Furthermore, the rapid disappearance of the keto form of $oxac^{2-}$ via parallel enolization and decarboxylation paths provides a time window through which it is possible to observe the reactions of the short-lived decarboxylation product, $Cu(pyr)_{enolate}$. The concentration changes which occur during the early stages of the reaction have been calculated by numerical integration, using the rate constants given in Table I, and are shown in Figure 5. The conditions chosen were such as to minimize paths involving uncomplexed $oxac^{2-}$; an excess of Cu^{2+}, 0.025 M, over total oxac, 0.001 M, at pH 3.4 was assumed. These reaction conditions approximate those used in obtaining the data points shown in Figure 1. The equations employed in performing this interion are given in the Appendix.

It is seen in Figure 5 that the concentration of $Cu(oxac)_{keto}$, which is the predominant form of $oxac^{2-}$ at zero time, rapidly decreases to a steady state value in 10-15 s. Concurrently, the concentrations of the enol and enolate complexes of $oxac^{2-}$ and $Cu(pyr)_{enolate}$ increase. The latter complex reaches a maximum concentration in about 2 s, then decreases to a steady state value in about 30 s. The rate of pyruvate formation becomes appreciable in about 1 s and reaches a maximum value in about 2 s. During the initial reaction stages this last rate was experimentally observed indirectly by measuring the decrease in absorbance of the acid form of methyl orange. The decrease is coupled to the H^+ change that accompanies pyruvate formation. An inflection point in the pyruvate formation curve is seen in Figure 5 to occur at about 2 s after a small amount of pyruvate has been formed. It was virtually impossible to observe this inflection owing to the relatively small change in absorbance observed at this time compared to the noise level in the stopped flow measurement. It was, however, established that the methyl orange absorbance remains essentially invariant for about 0.2-0.3 s after mixing, roughly in agreement with the predictions. At longer times (>30 s) the concentrations of $Cu(oxac)_{keto}$ and $Cu(pyr)_{enolate}$ have decreased to their steady state values, and the reaction stoichiometry essentially consists of the conversion of $Cu(oxac)_{enol}$ to Cu(pyr). In this region, shown in the right-hand side of Figure 5, where a change has been made in the time scale, the kinetics resemble those observed with Zn(II).

Earlier it had been found that enolization of $Zn(oxac)_{keto}$ proceeds via proton catalyzed, acetic acid catalyzed, and acetate catalyzed paths.[18] In this study we have uncovered a proton catalyzed path for the enolization of $Cu(oxac)_{keto}$ but have not been able to define the buffer catalyzed paths owing to the low acetate levels which were employed. The rate constants for the proton catalyzed enolization pathways are not greatly sensitive to the $oxac^{2-}$ environment. A definite, but relatively small, trend in the second-order rate constants is shown: $oxac_{keto}^{2-}$ > $Zn(oxac)_{keto}$ > $Cu(oxac)_{keto}$. The small influence of the metal ion on this proton catalyzed path may arise from opposing effects of coordination: a decreased tendency of the carbonyl oxygen atom to accept a proton owing to Coulombic repulsion by the metal ion vs. metal ion stabilization of the fraction of enol content that comprises the activated complex. The rates of the uncatalyzed enolization paths follow the reverse order as proton catalysis: $Cu(oxac)_{keto}$ > $Zn(oxac)_{keto}$ ≫ $oxac_{keto}^{2-}$. This order is the same as that of the enol contents of these species at equilibrium, providing further evidence for a connection between enol stabilization and reaction rates.

Gelles and Salama[13] observed that the ability of various metal ions to promote decarboxylation closely parallels the stabilities of their respective oxalate complexes. Because of the formal resemblance of oxalate to pyruvate enolate they proposed that metal ion activation has its origins in the stabilization of the intermediate rather than from polarization or weakening of the $oxac^{2-}$ carbon–carbon bonds. The results of the present investigations are consistent with this interpretation. For the two cases studied, the rate constants for the uncatalyzed enolization paths of the $M^{II}oxac^{2-}$ complexes parallel the decarboxylation rate constants, and they also parallel the equilibrium constants for enol formation. Thus, the higher the affinity of the metal ion for enol and enolate, the faster is the rate of decarboxylation. Another manifestation of this relationship is the ability of Cu(II), which has a high decarboxylation rate constant, to stabilize intermediate $Cu(pyr)_{enolate}$. While enol stabilization appears to promote a high decarboxylation rate constant, the parallel reaction, which reduces the proportion of keto form available for decarboxylation, opposes this. Therefore, a "leveling effect" occurs between the slow CO_2 evolution rates observed for different metal ions. Although these rates do differ, the differences are not as great as the inherent differences in their true decarboxylation rate constants.

The effective decarboxylation rate constants that apply to slow CO_2 evolution are equal to the product, $k_{-CO_2} \times f_{keto}$, where k_{-CO_2} is the true rate constant and f_{keto} is the fraction of Moxac that is present in the keto form. For a fast preequilibrium enolization f_{keto} is equal to the quotient $1/(1 + K_{enol})$. Gelles and his co-workers[12,13] attempted to correct their effective rate constants obtained from CO_2 evolution studies by using enol contents determined for metal ion-4-methyl oxaloacetate solutions. However, the extent of enolization they report for the ester-Cu(II) and Zn(II) reaction mixtures is considerably less than we have found for $oxac^{2-}$.

Any intrinsic chemical effects of the ester group on enolization aside, there are two reasons which could account for the lower ester results. Since $oxac_{enol}^{2-}$ appears to behave as a ligand in which both carboxylate groups are actively engaged in coordination, blocking one of these sites will remove a function that helps to stabilize the enol forms, **4a, b, c,** with respect to the keto form, **1.** Secondly, the stabilities of the complexes of the bidentate 4-ester derivative are probably comparable to those of pyruvate, or lactate. Under the dilute conditions employed by Gelles and Hay[12] extensive complex dissociation would occur giving rise to appreciable concentrations of the uncomplexed ligand, thereby, also, reducing the amount of enol in solution.

These factors combined with the mathematical characteristics of reversible first-order reactions could also account for the faster enolization rates observed by Gelles and Hay[12] for the 4-ethyl ester. In a set of reactions for which the forward rate constants remain somewhat constant (as appears to be the case with these ligands), those reactions which do not go to completion will show larger apparent backward rate constants, and consequently shorter relaxation times than those which do. This last effect results from the fact that the observed relaxation rate constants is the sum of the forward and backward rate constants. Thus, while the 4-ethyl derivate of $oxac^{2-}$ appears to be a very good qualitative model for $oxac^{2-}$ reactions in general, it may not be a good quantitative model for the reactions of $oxac^{2-}$ that involve metal ions.

In earlier work Speck[6] has shown that metal ion inhibition of decarboxylation occurs at high Cu(II). The results presented in Figure 4 verify this observation and also show that inhibition is pH dependent. Qualitatively, these data indicate that inhibition arises from the formation of polynuclear $Cu(II)\text{-}oxac^{2-}$ complexes. Quantitatively it was found not possible to account for the results shown in Figures 3 and 4 using a model in which inactivity is attributed to mononuclear complexes such as $CuH_{-1}oxac^{-}$, or the kinetically equivalent, $CuOHoxac^{-}$, but inclusion of $Cu_2H_{-1}oxac^{+}$ in addition to the potentiometrically observed $Cu_2H_{-2}oxac_2^{2-}$ gives a satisfactory fit.

The former complex has a composition similar to that of the dinuclear complex which was found to be responsible for metal ion inhibition in the $Zn(II)\text{-}oxac^{2-}$ system.[18] Possibly owing to the square-planar coordination behavior of Cu(II), this dinuclear species easily acquires another enolate ion to form a dimeric complex having the possible structure shown below.

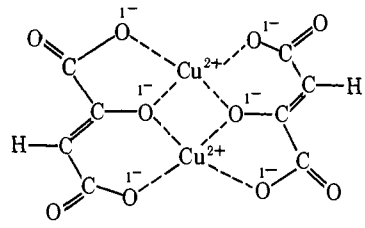

An alternate structure, which is indistinguishable solely through the pH dependence observed here, is one in which the ligand enol protons are retained and hydroxyl bridges join the Cu(II) atoms. We favor the dimeric enolate structure on the basis of the observed high stability of the complex and by analogy to similar species observed with malate[28] and parapyruvate.[29] Hydroxyl bridged Cu(II) dimers usually do not form below pH 6 at the concentration levels employed in this work, whereas, the potentiometric titration data shown in Figure 2 as well as the rate inhibition shown in Figures 3 and 4 indicate extensive formation of the unreactive dimers at pH 5.0 and below. Furthermore, the stability constant calculate on the basis of the formula $Cu_2H_{-2}oxac_2^{2-}$ is consistent with those found for other alkoxy bridged Cu(II) complexes. This can be seen in the values calculated for the exchange constants of the reactions,

$$Cu_2H_{-2}oxac_2^{2-} + 2CuL \rightleftarrows Cu_2H_{-2}L_2 + 2Cu(oxac) \quad (3)$$

The respective exchange constants of $oxac^{2-}$ for malate[28] and parapyruvate[29] are calculated to be $10^{-0.02}$ and $10^{-0.18}$. The proximity of these exchange constants to unity suggests that coordination through similar kinds and numbers of donor groups occurs on both sides of the equation.

Rough experiments on the rate of formation of the Cu(II)-malate dimer show that equilibration occurs well within the time scale of the rates investigated in this work. This substantiates the tacit assumption that the rate limiting step in forming the dinuclear $Cu(II)\text{-}oxac^{2-}$ complexes is the enolization rate of $oxac^{2-}$.

Finally, Steinberger and Westheimer[11] found that metal ions at high pH inhibit the decarboxylation of α,α-dimethyloxaloacetate, which cannot form an enolate complex. We propose that analogous dinuclear complexes are formed by displacement of an ^{-}OH proton from the hydrated form of the ligand, $^{-}O_2CC(OH)_2C(CH_3)_2CO_2^{-}$. Although, this hydrate resembles malate, it likely forms slightly less stable complexes owing to the fact that the free ligand is only fractionally hydrated.

Appendix

The following equations were used in obtaining the curves shown in Figure 5.

$$-\frac{d\mathrm{Cu(oxac)_{keto}}}{dt} = (k_4[H^+] + k_5 + k_{-CO_2}) \times [\mathrm{Cu(oxac)_{keto}}] - (k_{-4}[H^+] + k_{-5}) \times f_{\mathrm{Cu(oxac),enol}}[\mathrm{Cu(oxac)_{enol}}]_{tot}$$

$$\frac{d[\mathrm{Cu(oxac)_{enol}}]_{tot}}{dt} = (k_4[H^+] + k_5)(\mathrm{Cu(oxac)_{keto}}) - (k_{-4}[H^+] + k_{-5}) f_{\mathrm{Cu(oxac),enol}}[\mathrm{Cu(oxac)_{enol}}]_{tot}$$

$$\frac{d\mathrm{Cu(pyr)_{enol}}}{dt} = k_{-CO_2}[\mathrm{Cu(oxac)_{keto}}] - k_H[\mathrm{Cu(pyr)_{enolate}}]$$

$$\frac{d\mathrm{Cu(pyr)}}{dt} = k_H[\mathrm{Cu(pyr)_{enolate}}]$$

$$[\mathrm{Cu(oxac)_{enol}}]_{tot} \sim [\mathrm{Cu(oxac)_{enol}}] + [\mathrm{Cu_2H_{-1}oxac^+}]$$

A fourth-order Runge-Kutta procedure was used to perform the numerical integration

References and Notes

(1) We wish to express our gratitude to the National Science Foundation for the support of this research.
(2) L. Krampitz and C. Werkman, *Biochem. J.*, **35**, 595 (1941).
(3) A. Krebs, *Biochem. J.*, **36**, 303 (1942).
(4) A. Kornberg, S. Ochoa, and A. Mehler, *J. Biol. Chem.*, **174**, 159 (1948).
(5) P. M. Nossal, *Aust. J. Exp. Biol. Med. Sci.*, **26**, 531 (1948).
(6) J. Speck, *J. Biol. Chem.*, **178**, 315 (1949).
(7) S. Seltzer, G. A. Hamilton, and F. H. Westheimer, *J. Am. Chem. Soc.*, **81**, 4018 (1959).
(8) G. W. Kosicki and F. H. Westheimer, *Biochemistry*, **71**, 4303 (1968).
(9) F. H. Westheimer, XVth Robert A. Welch Foundation Conference on Chemical Research, Nov. 1-3, 1971, p 7.
(10) K. J. Pederson, *Acta Chem. Scand.*, **6**, 285 (1952).
(11) R. Steinberger and F. H. Westheimer, *J. Am. Chem. Soc.*, **73**, 429 (1951).
(12) E. Gelles and R. W. Hay, *J. Chem. Soc.*, 3673 (1958).
(13) E. Gelles and A. Salama, *J. Chem. Soc.*, 3864, 3689 (1958).
(14) G. W. Kosicki and S. N. Lipovac, *Can. J. Chem.*, **42**, 403 (1964).
(15) J. V. Rund and R. A. Plane, *J. Am. Chem. Soc.*, **86**, 376 (1964).
(16) E. Bamann and V. S. Sethi, *Arch. Pharm. (Weinheim, Ger.)*, **301**, 78 (1968).
(17) K. G. Claus and J. V. Rund, *Inorg. Chem.*, **8**, 59 (1969).
(18) W. D. Covey and D. L. Leussing, *J. Am. Chem. Soc.*, **96**, 3860 (1974).
(19) N. V. Raghavan and D. L. Leussing, *J. Am. Chem. Soc.*, **96**, 7147 (1974).
(20) G. Schwarzenbach and H. Flaska, "Complexometric Titrations", 2nd English ed, Nethven and Co. Ltd., London, 1969.
(21) I. M. Kolthoff, *J. Phys. Chem.*, **34**, 1466 (1930).
(22) Proton magnetic resonance experiments performed in our laboratories show that the decarboxylation of Zn(oxac) in the presence of pyruvate induces the formation of parapyruvate. B. J. Lillis and D. L. Leussing, submitted for publication; in unpublished experiments N. V. Raghavan has shown that products having an intense absorption in the uv are formed when Cu(oxac) is decarboxylated in the presence of pyruvate. This absorption is characteristic of Cu(II)-parapyruvate complexes.
(23) A. Meister, *J. Biol. Chem.*, **184**, 117 (1950).
(24) S. S. Tate, A. K. Grzybowski, and S. P. Datta, *J. Chem. Soc.*, 1372 (1964).
(25) J. L. Hess and R. E. Reed, *Arch. Biochem. Biophys.*, **153**, 226 (1972).
(26) The $Zn(II)$-$oxac^{2-}$ data have been recalculated by W. D. Covey of our laboratories. Inclusion of a noncatalyzed reaction path for the reaction of $Zn(oxac)_{keto}$ does, indeed, give a better fit to the data, with only minor changes from the rate constants originally reported.[18] The new values are given in Table I.
(27) L. G. Sillen and A. E. Martell, *Chem. Soc., Spec. Publ.*, **No. 17**, (1964); **No. 25** (1971).
(28) K. S. Rajan and A. E. Martell, *J. Inorg. Nucl. Chem.*, **29**, 463 (1967).
(29) N. V. Raghavan, unpublished results.

Ternary Complexes in Solution. XXIV.[1] Metal Ion Bridging of Stacked Purine–Indole Adducts. The Mixed-Ligand Complexes of Adenosine 5′-Triphosphate, Tryptophan, and Manganese(II), Copper(II), or Zinc(II)

Helmut Sigel* and Christoph F. Naumann

Contribution from the Institute of Inorganic Chemistry, University of Basel, CH-4056 Basel, Switzerland.

Received May 5, 1975

Abstract. The stability constants of the mixed-ligand complexes containing ATP, tryptophan (Trp), and Mn^{2+}, Cu^{2+}, or Zn^{2+} (= M) were determined from potentiometric titrations. The stability of complexes is characterized by $\Delta \log K_M = \log K^{M(ATP)}_{M(ATP)(Trp)} - \log K^{M}_{M(Trp)}$, which corresponds to the equilibrium, $M(ATP)^{2-} + M(Trp)^{+} \rightleftharpoons M(ATP)(Trp)^{3-} + M^{2+}$. A comparison of these data with those of the corresponding complexes containing alaninate instead of tryptophanate reveals an increased stability (about 0.2 to 0.6 log unit) of the ternary complexes formed with tryptophanate. This gave the first hint of an intramolecular stacking between the indole and purine moieties in these mixed-ligand complexes; i.e., these complexes can be considered as metal ion bridged stacking adducts. In fact, uv-difference absorbance studies revealed a new absorbance in the 295-nm region which could be attributed to an indole-purine interaction in these ternary complexes by comparison with systems containing only tryptophan and either adenosine or ATP. Changes in the ^1H NMR spectrum of the Zn^{2+}-ATP-Trp system confirmed that the aromatic moieties are linked together by the coordination of a metal ion to the phosphate chain of ATP and the amino acetate part of tryptophan. The extents of formation of the ternary complexes, $M(ATP)(Trp)^{3-}$, were calculated. The factors favoring their formation (e.g., the oxidation of Mn^{2+} to Mn^{3+}) and the structure of their folded form are discussed. Possible biological implications are outlined taking into account systems in which the coenzyme and the activating metal ion bind less well to the enzyme than does the coenzyme-metal ion complex.

It is now well established[2,3] that charge-transfer interactions may play a major role in biological systems. Examples are the interactions of adenine coenzymes and glutamate dehydrogenase,[4] creatine kinase,[5] octopine dehydrogenase,[6] or myosin,[7] where stacking between the adenine moiety of the coenzyme and an aromatic amino acid residue has been suggested. Among the side chains of amino acids, the indole moiety is the most potent electron donor.[8] Indeed, charge-transfer-type interactions between tryptophan or other indole derivatives and nucleosides or nucleotides occur in aqueous solution.[9-12] However, purine and pyrimidine bases can also stack with each other,[13] and this contributes to the stability of nucleic acid helices.[14]

In general, the stability of such adducts is small, unless